Applied Catalysis B: Environmental 99 (2010) 235–241

Contents lists available at ScienceDirect

Applied Catalysis B: Environmental

journal homepage: www.elsevier.com/locate/apcatb

The effect of $C_{(s)}$ on the trapping of NO_x onto $Pt/Ba/Al_2O_3$ catalysts

James A. Sullivan*, Petrica Dulgheru

UCD School of Chemistry and Chemical Biology, SFI SRC in Solar Energy Conversion, Belfield, Dublin 4, Ireland

ARTICLE INFO

Article history:
Received 19 February 2010
Received in revised form 11 June 2010
Accepted 17 June 2010
Available online 25 June 2010

Keywords:
NO_x trap
Particulate combustion
4-Way catalysis

ABSTRACT

$Pt/BaO/Al_2O_3$ catalysts react with NO/O_2 mixtures to form barium nitrites and nitrates. In the presence of small amounts of $C_{(s)}$ admixed with the catalyst the concentrations of NO_x adsorbed is considerably reduced and the stability of the stored NO_x is decreased. These results suggest that there are important implications for any attempts to combine NSR and particulate combustion systems within a single catalytic system. Furthermore, it is clear that there are significant concentrations of mobile NO_x species present in the environs of the NO_x trap prior to fixation on BaO, *i.e.* the transfer between NO_2 formed on the Pt component of the trap and the "fixed" NO_x in $Ba(NO_3)_2$ involves significant concentrations of gaseous or surface mobile NO_2.

1. Introduction

NO_x and Particulate Matter (PM) are two of the more intractable pollutants emitted from diesel engine exhausts [1–3]. NO_x contributes to photochemical smog and acid rain while PM can be carcinogenic and also contributes to global warming through decreasing the albedo of Arctic and Antarctic ice. Neither is removed from the exhaust stream using conventional 3-way catalysts and other technologies are required.

Currently within exhaust gases of a net oxidising nature, NO_x is reduced to N_2 using NO_x Storage and Reduction (NSR) technology where NO is trapped on BaO forming $Ba((NO)_3)_2$. Once the trap is saturated a pulse of hydrocarbons over the material reacts to release NO, regenerate the BaO sorbent material and reduce the NO to N_2 [4–10]. The first step in this cycle is the oxidation of NO (over Pt) to form NO_2 [11,12].

Removal of particulates can take place in a somewhat related system (the Diesel Particulate Filter—DPF) where particles are trapped in the pores of adapted monoliths. These have alternate ends plugged forcing the exhaust gas through the walls of the monolith where larger particles are trapped [13–15]. In the case of continuous regeneration systems, trapped particles are burned off using either a periodic high temperature oxidation in air or through a lower temperature reaction with NO_2.

In the latter case NO, present in the exhaust gas (in combination with a suitable NO oxidation catalyst), promotes soot combustion through the formation of NO_2 which then reacts with $C_{(s)}$ transferring an O atom and regenerating NO [16–17].

Since the oxidation of NO is a primary step both in the trapping onto an NSR material and the promotion of soot combustion on a DPF, the attempt to combine both of these technologies into a single catalytic bed seems obvious. Furthermore, it has been reported that the presence of a NSR system improves particulate removal from diesel exhausts [1,18–20]. Previously [21], we have shown that the reason for this improved activity is related to the increased transient concentration of NO_x present during regeneration of the NSR material rather than to any inherent catalytic activity in the components of the NSR material.

In the same article we showed that the presence of $C_{(s)}$ has a detrimental effect on the ability of a model $Pt/BaO/SiO_2$ material to store NO_x once exposed to NO/O_2 mixtures at 400 °C. This obviously has an effect on the application and operation of the NO_x trap in terms of the frequencies of regenerations that would be required if trap capacities fell. This in turn has an effect on the fuel efficiency of any vehicle that operates such a system.

While several groups have studied the effect of NO_x (and NO_x trapping materials) on soot combustion [18–23] very few have studied systematically the reverse interactions, *i.e.* the effect of soot on the activity and capacity of a NO_x trap. Kustov and Makkee [23] have reported the presence of soot destabilizes NO_x storage on Sr-containing NSR materials and Matarrese at al. [22] have reported that the presence of soot at relatively low levels (catalyst: soot ratios > 10:1) does not affect the trapping capacities of model

* Corresponding author. Tel.: +353 1 7162135.
E-mail address: James.Sullivan@ucd.ie (J.A. Sullivan).

0926-3373/$ – see front matter © 2010 Elsevier B.V. All rights reserved.
doi:10.1016/j.apcatb.2010.06.025

Ba-containing NSR systems, while higher soot loadings (catalyst: soot = 4:1) do have a detrimental effect and Kustov and Makkee [23] have reported the presence of soot destabilizes NO_x storage on Sr-containing NSR materials.

In the current work we study this detrimental effect of $C_{(s)}$ on NO_x storage in more detail using Al_2O_3 supported NSR materials. Specifically, we use Al_2O_3 to attempt to see whether the temporary storage of NO and NO_2 on the surface of Al_2O_3 (a process not possible over SiO_2 supported materials) has any effect on the problems seen previously. We also look at the effects that (a) $C_{(s)}$ concentrations in a catalyst-soot mixture and (b) the length of time that such mixtures are exposed to NO/O_2 gas mixtures have on the concentrations and stability of adsorbed (trapped) NO_x. Transient gas switching techniques (studying the dose of $NO + O_2$ onto the catalyst) and Temperature Programmed Desorption (studying the removal of adsorbed NO_x from the catalyst) are the tools used to probe these features. Our results concur with those reported in [23] in that the effect noted over Sr materials was reproduced here over Ba-containing materials while they contrast somewhat with [22] as in our situation the presence of even minor amounts of soot (catalyst:soot ratio = 50:1) have a dramatic effect on the NO_x storage capacities.

2. Experimental

2.1. Catalyst preparation

The catalyst used in this study was a 1% Pt/10% BaO/Al_2O_3 material. The Pt precursor was a Pt acetylacetonate (acac), $Pt(CH_3COCHCOCH_3)_2$ while the BaO was derived from barium acetate. Both salts were provided by Aldrich. γ Al_2O_3 supports were provided by Johnson Matthey and had a surface area of 210 $m^2\,g^{-1}$. The material was prepared through incipient wetness impregnation. In the first step the Al_2O_3 was crushed and sieved to particle sizes 212–600 μm before aliquots were repeatedly loaded with aqueous solutions containing sufficient barium acetate to eventually result in a 10% BaO loading. The material was dried at 80 °C before being calcined for 2 h at 500 °C. Subsequently the powder was loaded with a Pt acetylacetonate (acac), $Pt(CH_3COCHCOCH_3)_2$ solution in CH_3NO_2 of sufficient concentration to result in a 1% loading. This powder was subjected to the same drying/calcination treatment as above.

Printex U (Degussa) is a commercial Carbon Black and was used as a model soot. The properties of Printex U have been previously described [24]. Catalyst–soot mixtures were prepared in varying ratios as follows. The catalyst (1 g 1%Pt/10% BaO/Al_2O_3) was mixed with 0–200 mg of soot in different catalyst to soot ratios. After the required masses of catalyst and soot were weighed they were transferred to a glass vial and mixed for about 1 min using a spatula. This approximates a loose contact situation (similar to the one in a diesel particulate filter). Accurately weighed aliquots of these mixtures were subsequently used in TPD experiments.

2.2. NO/O_2 adsorption step and temperature programmed desorption

The catalysts (50 mg of catalyst or catalyst: soot mixture) were loaded into a tubular reactor (OD 8 mm) and held in place using two plugs of quartz wool. The mass of all catalyst:soot mixtures was chosen such that 50 mg of catalyst was present in the reactor. The reactor was placed in a furnace connected to a gas handling system. The catalyst was initially held in a flow of He (100 mL min^{-1}) and the temperature was raised from room temperature to 400 °C. It was held at this temperature for a brief period (10 min) before the $NO + O_2$ dose commenced. The NO was taken from a certified cylinder of 1% NO/He (BOC) while the He and O_2 were taken from high purity O_2 and He cylinders also provided by BOC. The flow rates of the individual gases were controlled using Bronkhorst mass flow controllers powered by an in-house constructed power supply.

The gas handling system was designed in such a way that a He flow (100 mL min^{-1}) over the catalyst could be replaced (through actuation of an electronically controlled valve) with a stream that contained a mixture of NO (2000 ppm), O_2 (10%) and He while retaining the same overall flow (100 mL min^{-1}). This mixture flowed over the catalyst for a defined amount of time (60, 300 or 600 s) before being replaced once more with the pure He stream. During these doses the catalyst was contacted with (160, 800 and 1600 μmol NO g^{-1} respectively). Recall that the catalyst composition used (1% Pt/10% BaO/Al_2O_3 contains 730 μmol Ba g^{-1} resulting in a theoretical NO_x trapping capacity assuming that all Ba atoms are available to act as a NO_x store (through the formation of $Ba(NO_3)_2$) of 1460 μmol NO g^{-1}. During these experiments the mass spectrometer monitored fragments at m/z = 4, 16, 17, 18, 22, 28, 30, 32, 44 and 46. The relevant profiles were (following suitable corrections due to fragmentation overlaps) converted to units of concentration and plotted as a function of time. Specifically, regarding treatment of the NO and NO_2 profiles the contribution of NO_2 to the NO signal at m/z = 30 was removed (through a knowledge of the cracking patterns of NO_2 within the mass spectrometer [25]) before the NO signal was converted to ppm. NO_2 profiles were converted to ppm through calibration plots at m/z = 46.

Comparison of m/z = 44 profiles with those of m/z = 28 and 12 suggest N_2 or N_2O formation during the dose periods or subsequent TPD experiments is minimal, *i.e.* the m/z = 12 and 28 profiles mirror that for m/z = 44 (suggesting that the bulk of the signal from m/z = 44 derives from CO_2). Similarly the m/z = 14 (N) signal mirrors those of m/z = 30 ($NO + NO_2$) and m/z = 46 (NO_2). This does not rule out the formation of minor amounts of N_2 or N_2O.

At this time the reactor was cooled to 200 °C in the He flow. This cooling took approximately 10 min. After the mass spectrometer readings had returned to the baseline values the TPD protocol was commenced. The temperature of the catalyst was ramped at a rate of 20 °C min^{-1} between 200 °C and 750 °C while the exit gases were continuously monitored by Mass Spectrometry (Prolab) and the fragments at m/z = 4, 16, 17, 18, 22, 28, 30, 32, 44 and 46 were recorded. As above, the outputs were converted into concentration units and plotted in TPD profiles as a function of temperature.

3. Results and discussion

Fig. 1 shows the NO, NO_2 and NO_x profiles measured at the exit of the reactor during different exposures (60 s, 300 s and 600 s) of 1% Pt/10% BaO/Al_2O_3 catalyst to $NO + O_2$ mixtures at 400 °C. The $NO + O_2$ mixture is switched into the reactor at 1 min and removed at 2, 6 and 11 min, respectively. The profiles relating to the 60 s dose are the lower three, the 300 s dose the middle three and the 600 s dose the upper 3 curves.

It is clear that only a very small amount of NO_x leaves the reactor during the first minute of the dose, *i.e.* the vast majority of the incoming NO_x is trapped on the catalyst. Following this, breakthrough takes place and NO and NO_2 (NO_x) begins to appear in the exit stream. As expected, its concentration rises with additional time. After 5 min of $NO + O_2$ dosage, the NO level is approximately 2000 ppm.

When each dose is completed and the $NO + O_2$ is removed from the stream the measured NO level (but not the NO_2 level) actually increases for over 1 min (NO was removed at minutes 2, 6 and 11 of the plots) before it (and the overall NO_x level) falls back to background levels. This shows that the NO_x species

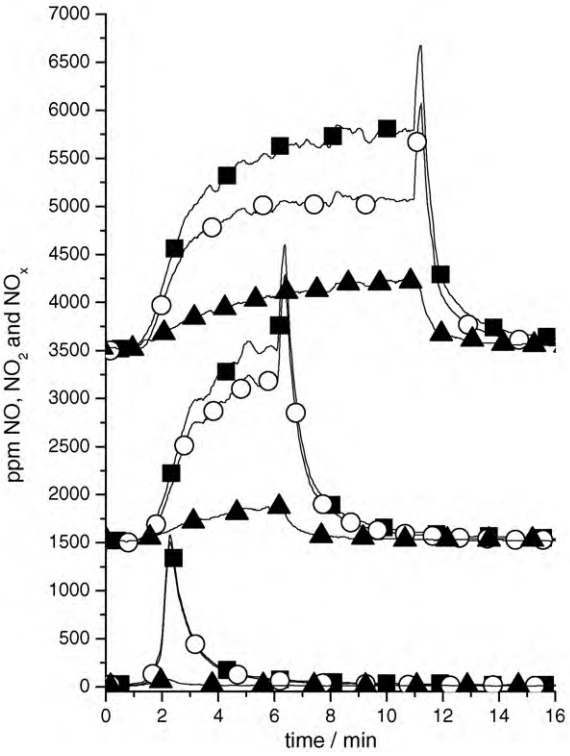

Fig. 1. NO, NO_2 and NO_x profiles during the dose (at 400 °C) of 1% Pt/10% BaO/Al_2O_3 with NO (2000 ppm) + O_2 (10%) for 60 s (lower plots), 300 s (middle plots) and 600 s (upper plots). NO (O), NO_2 (▲), NO_x (■) In all cases the NO + O_2 was switched into the stream at 1 min. Once the NO + O_2 is removed from the stream the catalyst is cooled to 200 °C—a process that takes ~10 min.

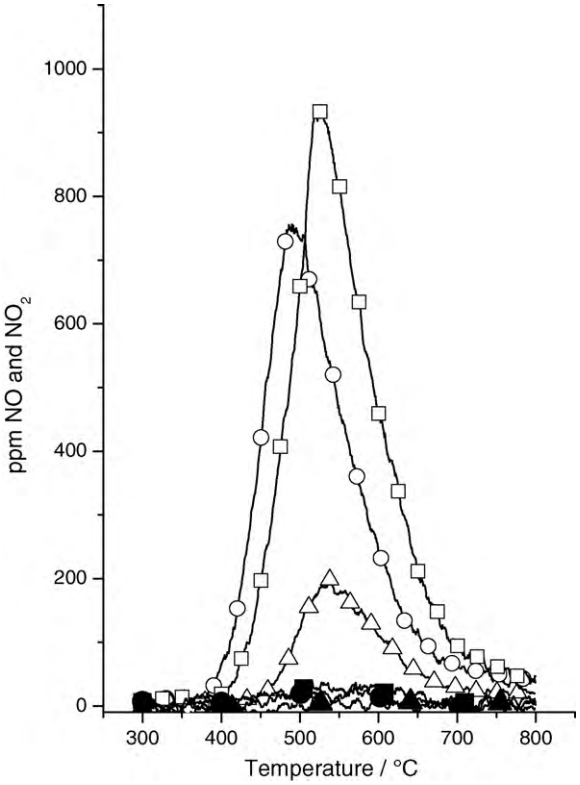

Fig. 2. Temperature programmed desorption profiles following the NO + O_2 treatments detailed in Fig. 1. NO—empty symbols, NO_2—filled symbols. Dose times—60 s (△, ▲), 300 s (○, ●), 600 s (□, ■). Samples were held in a flow of He while the temperature was ramped to 750 °C at 20 °C min^{-1}.

adsorbed at 400 °C in the presence of NO and O_2 were unstable during the cooling process in the inert atmosphere. This may indicate a partial decomposition of $Ba(NO_3)_2$ which is unstable in the inert atmosphere (although bulk $Ba(NO_3)_2$ is stable in inert atmospheres to far higher temperatures) or to the removal of NO_x species stored on the Al_2O_3 surface. This effect, *i.e.* the release of amounts of NO_x from the storage material once gaseous NO had been removed from the inlet stream has been seen before (albeit in the absence of cooling) in reference [26] and ascribed to these possibilities.

However, the fact that the NO_x released is solely NO and not NO_2 suggests disproportionation of NO_{2ads} to NO_{3ads} and NO_{ads} and this NO (being unstable on the surface at the catalyst temperature) desorbs from the surface. The generation of NO from NO_2 during the loading of a NO_x trap has been previously seen and explained in these terms [27–30]. Another feature to note is that the subsequent TPD measurements show NO_x (predominantly NO accompanied by O_2) desorption commences at temperatures below the dose temperature of 400 °C (see below). This points to substantial reorganisation within the NO_x adsorbed layer, *i.e.* the NO/NO_2 which was stable enough to remain on the surface at 400 °C and during the cooling phase had reacted in some way (during the latter) to become unstable at 400 °C.

CO_2 is also released from the NSR materials once they are exposed to NO + O_2 at 400 °C. This arises from the displacement of $BaCO_3$ during the formation of $Ba(NO_3)_2$ and has been seen several times previously *e.g.* in [26]. The $BaCO_3$ arises both during the calcination of Barium acetate (where formed CO_2 reacts with surface BaO at high temperatures) and the adsorption of atmospheric CO_2 during storage of the material. A plot showing the mass spectrometer response at $m/z = 44$ following the inlet of NO + O_2 in following a typical switch is shown in Supporting Information (S1). This also shows the $m/z = 44$ profile from an analogous switch in the presence of $C_{(s)}$—see later.

Fig. 2 shows the resulting NO_x TPD profiles obtained when these materials are subjected to a temperature ramp (in He) to 750 °C at a rate of 20 °C min^{-1} after being cooled in He (to 200 °C) following the NO + O_2 dose. In all cases NO was the predominant form of NO_x desorbed (higher profiles). Minor (unquantifiable using our analysis conditions) amounts of NO_2 were seen from samples (lower three profiles in Fig. 2) which had been dosed for 10 min. These results are similar to the results seen by Nova et al. [26] and, in their case the lack of large amounts of NO_2 was ascribed to the rapid decomposition of any desorbed NO_2 before it left the reactor. In all cases the NO was accompanied by a release of O_2 (see Supporting Information Figure S2 for an example). At higher temperatures CO_2 desorption is also seen. These desorptions (shown in S3) relate to the decomposition of $BaCO_3$ and interestingly more CO_2 desorbs from samples which had been dosed for lower times in NO + O_2—suggesting, not unreasonably, that proportionately less CO_2 had been desorbed from the NO_x storage materials during these doses.

In the case of the sample dosed in NO + O_2 for 60 s the desorption of NO begins at 440 °C, reaches a maximum at 550 °C and is complete by 720 °C. In total 131 μmol g^{-1} of NO was released during TPD. In the case of the sample dosed in NO + O_2 for 300 s NO begins to desorb at 350 °C, reaches a maximum at 480 °C and is complete at approximately 730 °C. During this TPD 402 μmol g^{-1} NO are desorbed. Samples dosed in NO + O_2 for 600 s began to desorb NO at approximately 380 °C with the desorption reaching a maximum at 520 °C. More NO_x is desorbed during this TPD (521 μmol g^{-1}). The temperatures of desorption are similar to those seen previously for the decomposition of surface and bulk $Ba(NO_3)_2$ [31,32]. These results indicate that the initial NO_x dosed onto the catalyst "finds"

very stable sites on which to adsorb (given that the temperature of maximum desorption and the initial temperature of desorption can be taken as a measures of stability) and also that most of the easily accessible sites are saturated following a 5 min dose, *i.e.* doubling the dose time to 10 min increases the [NO_x] adsorbed only by approximately 25%. In terms of the proportion of BaO utilized during the NO_x trapping experiments the dose at 60 s utilizes approximately 9% of the Ba while those lasting for 300 and 600 s utilize approximately 27% and 36% respectively. This confirms that there are significant portions of BaO that are not available for NO_x trapping (presumably buried in the bulk of $BaCO_3$ particles) and this is consistent with previous observations of NO_x trapping capacity in related model systems [2,4,33].

Interestingly, for both of the longer dose times desorption of NO begins at temperatures below that at which the NO + O_2 dose was made. This indicates that material which remained on the surface following a dose at 400 °C were altered during the cooling phase, becoming less stable and eventually desorbed at a lower temperature than that at which they were initially held. This result, along with the desorption seen above in the absence of NO + $O_{2(g)}$ indicates a redistribution of the NO_x adsorbed onto the surface during the cooling in He between 400 and 200 °C where some less stable NO_x-containing species are formed.

The final interesting feature that should be discussed is the relative stabilities of the species remaining on the material following the doses for different times. It appears that the first adsorbed NO_x finds the most stable sites while the NO_x adsorbed after a 5 min dose is significantly less stable (in terms of temperature of maximum and initial NO desorption). Subsequently, following a 10 min dose the NO_x adsorbed shows intermediate stabilities according to the T_{max} and $T_{initial}$ criteria. This is reproducible behaviour and we ascribe the gain in stability of the NO_x adsorbed between 5 and 10 min doses to a dynamic equilibration of the formed surface nitrates with $NO_{(g)}$, $O_{2(g)}$ and $NO_{2(g)}$ during the extended dose.

Fig. 3 shows the NO, NO_2, NO_x and CO_2 profiles measured at the exit of the reactor during different exposures (60 s, 300 s and 600 s) of a mixture of 50 mg $Pt/BaO/Al_2O_3$ catalyst and 5 mg of Printex U (Degussa) soot to NO + O_2 at 400 °C (at the same concentrations as shown in Fig. 1). The breakthrough profiles for $NO/NO_2/NO_x$ are roughly comparable to the situations seen in the absence of soot however there are some differences in the composition of the NO_x. Here, much smaller amounts of NO_2 were noted during the dose period compared to those seen during the dose periods in the absence of soot. As an example, at the end of the 600 s dose before NO + O_2 is removed from the stream approximately 31% of the exit gas NO_x was NO_2 while in the same experiment in the presence of soot the proportion was approximately 6%. This indicates reaction of NO_2 with soot to form NO. All profiles again show the transient release of NO (not NO_2) once the NO + O_2 is removed from the stream (for the reasons outlined above) although this is a lot less pronounced than in the absence of soot.

CO_2 production begins immediately once NO + O_2 is introduced into the stream and production ceases once NO + O_2 is removed from the reactor inlet. This CO_2 arises from two sources, *i.e.* the decomposition of $BaCO_3$ and the combustion of the $C_{(s)}$ in the catalyst–soot mixture. The former source is important in the early portions of the switch (see Supporting Information S1) but the main source of the CO_2 observed following the initial decomposition of surface $BaCO_3$ is the combustion of $C_{(s)}$. In principle, the CO_2 profile from the 300 s dose should mirror exactly the first 300 s of the 600 s dose and in fact the shapes of the profiles are the same. However it seems that more CO_2 is produced in the latter experiment. This is more than likely due to inhomogeneity within the catalyst–soot mixture. In both cases a pseudo-steady-state conversion to CO_2 is

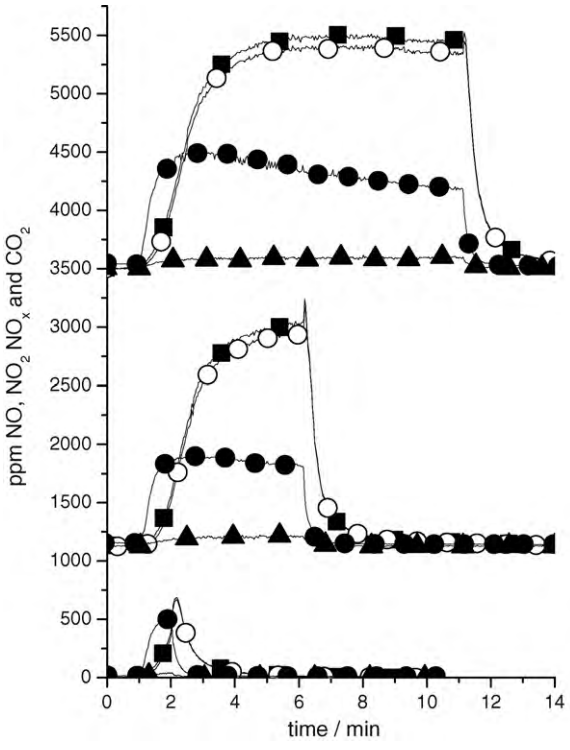

Fig. 3. NO, NO_2, NO_x and CO_2 profiles during the dose (at 400 °C) of 50 mg 1% Pt/10% BaO/Al_2O_3 mixed with 5 mg of Printex U soot with NO (2000 ppm) + O_2 (10%) for 60 s (lower plots), 300 s (middle plots) and 600 s (upper plots). NO (○), NO_2 (▲), NO_x (■), CO_2 (●). In all cases the NO + O_2 was switched into the stream at 1 min.

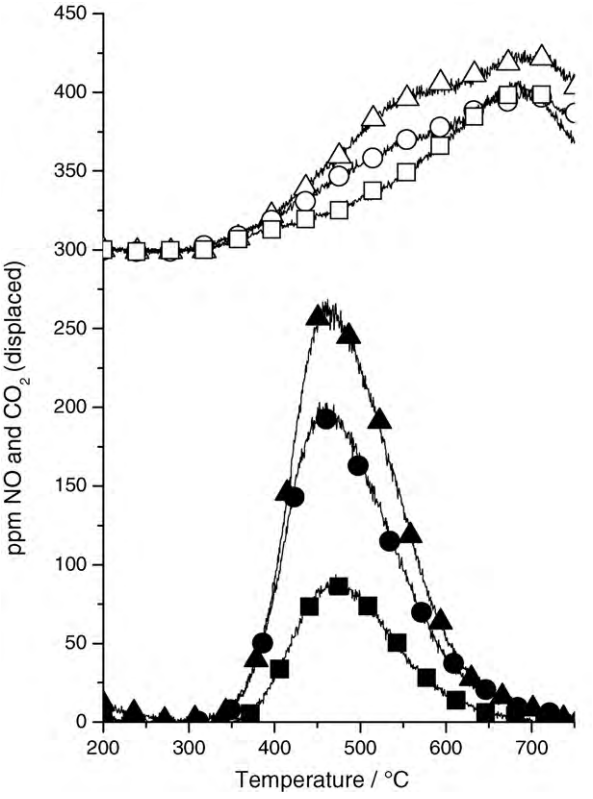

Fig. 4. NO (closed symbols) and CO_2 (open symbols—displaced) profiles during TPD following the dose shown in Fig. 3. Samples dosed in NO + O_2 for 60 s (■, □), 300 s (●, ○) and 600 s (▲, △).

Table 1
Absolute amounts of NO_x desorbed and the temperature of maximum NO_x desorption following a dose of 1% Pt/10% BaO/Al_2O_3 catalyst with NO (2000 ppm) + O_2 (10%) for various times with different catalyst:soot ratios. The numbers in parentheses indicate the fraction of the BaO present on the catalyst that was utilized during the trapping.

Dose time	60 s			300 s			600 s		
Catalyst:soot	NO_x desorbed/μmol g^{-1}	$T_{initial}$/°C	T_{max}/°C	NO_x desorbed/μmol g^{-1}	$T_{initial}$/°C	T_{max}/°C	NO_x desorbed/μmol g^{-1}	$T_{initial}$/°C	T_{max}/°C
∞	131 (9%)	440	550	402 (27%)	350	480	521 (35%)	380	520
50:1	40 (3%)	350	460	104 (7%)	330	460	133 (9%)	332	460
20:1	67 (5%)	350	465	145 (10%)	330	460	156 (11%)	330	450
10:1	62 (4%)	355	470	122 (8%)	325	460	137 (9%)	330	460
5:1	20 (1%)	350	480	76 (5%)	345	470	177 (12%)	320	450

reached roughly 2 min after the NO + O_2 is switched into the stream and this gradually decreases as the time of reaction increases.

Fig. 4 shows the CO_2 and NO temperature programmed desorption profiles obtained from the three catalyst–soot mixtures following these difference pre-treatments in NO + O_2. There was no evidence of any measurable N_2 formation through the course of any of the TPD (or NO + O_2 dose) measurements (the N fragment mirrors exactly the NO signal at $m/z = 30$). There was also no measurable NO_2 desorption although again there were O_2 desorptions accompanying the NO desorption. The first obvious feature to note is that the amount of NO_x (NO + NO_2) desorbed is significantly decreased relative to the same catalysts dosed under the same conditions in the absence of soot. The second feature is that the temperatures of initial and maximum desorption are lower in each case also (see Table 1, 4th row of data).

The CO_2 profiles are also of interest during these TPD measurements. CO_2 is seen from approximately the same temperature during the temperature ramp as NO. Its concentration increases with temperature (as does the concentration of NO). However, in the case of NO, once the surface concentration becomes the limiting factor in the development of the desorption profile, *i.e.* above T_{max}, the gas phase concentration decreases once more. This is not the case with the CO_2 profile which continues to rise, showing a shoulder at approximately 550 °C and reaching a maximum at approximately 680 °C. This profile can be explained by the decomposition of different types of $BaCO_3$ on the catalyst surface [33–36]. We cannot rule out a contribution from the reaction between liberated O_2 and $C_{(s)}$ (which can take place as long as gas phase O_2 is available) however, inspection of the oxygen derived peak (which is coincident with the NO desorption) and the CO_2 peak (the low temperature shoulder of which is not coincident with these maxima) suggests this feature is more likely to involve a thermal decomposition of $BaCO_3$.

This decomposition temperature is similar to those seen previously for the decomposition of surface $BaCO_3$ species [28–30]. There are two possible sources for the formation of this $BaCO_3$, *i.e.* atmospheric CO_2 picked up during or after the preparation of the catalyst, or CO_2 formed during the dose of the catalyst–soot mixture at 400 °C in NO + O_2. Comparisons of the CO_2 profiles shown here (following the dose in the presence of soot) with those seen during TPD of catalysts dosed with NO + O_2 in the absence of soot (Supporting Information Figure S3) suggest that significant portions of the decomposing $BaCO_3$ is formed from a BaO + CO_2 reaction at 400 °C during the dose in NO + O_2 where the CO_2 is formed from the oxidation of $C_{(s)}$ at this temperature, *i.e.* CO_2 profiles seen during the TPD of NO_x from catalysts dosed in the absence of soot are lower than in Fig. 4 above.

The effect of [$C_{(s)}$] was also studied and experiments were carried out where 50 mg of catalyst was mixed with different masses of $C_{(s)}$ ranging from 1 mg to 10 mg (resulting in catalyst:soot ratios of between 50:1 and 5:1. Table 1 compares the absolute amounts of NO_x desorbed and the temperature of maximum desorption for each experiment in the absence and the presence of 0–10 mg of soot (catalyst:soot ratios of between ∞ and 5:1). In all cases the absolute amount of NO_x desorbed is much decreased and the temperature of initial and maximum desorption falls in the presence of soot.

Fig. 5 shows the NO, NO_2 and CO_2 profiles seen during a 300 s dose of the catalyst in NO + O_2 in the presence of varying (1 mg, 2.5 mg, 5 mg and 10 mg) amounts of $C_{(s)}$ (the NO_x profiles (NO + NO_2) have been left out for clarity) while Fig. 6 shows the CO_2 and NO TPD profiles following this dose (again no NO_2 was noted during the TPD experiments). For reference in Fig. 5 the NO, NO_2 and CO_2 profiles relating to the 300 s dose of NO + O_2 onto the catalyst in the absence of $C_{(s)}$ are also shown. For reasons of clarity the respective TPD profiles from the latter experiment are not shown in Fig. 6.

From the profiles in Fig. 5 it is clear that the different concentrations of soot have a relatively small effect on the NO_x adsorption behaviour. Roughly equivalent NO breakthrough profiles are noted over 50 mg of catalyst mixed with 1, 2.5, 5 and 10 mg of soot. There is no correlation with this breakthrough time or levels and the amount of soot in the mixture, *i.e.* the shapes of the profiles are similar when 1 mg or 10 mg are admixed with the 50 mg of 1% Pt/10% BaO/Al_2O_3. At the completion of the 300 s dose, once the NO + O_2 is

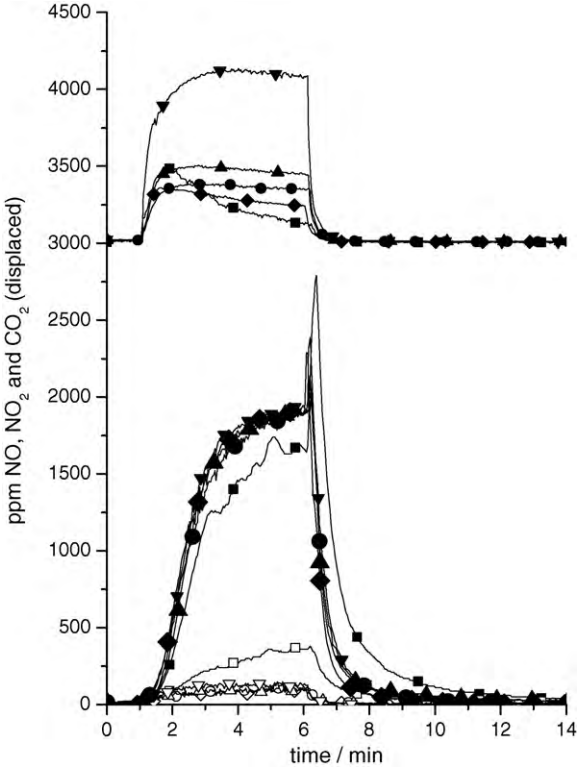

Fig. 5. NO and CO_2 (closed symbols) and NO_2 (open symbols) profiles during the dose of a mixture of 50 mg 1% Pt/10% BaO/Al_2O_3 and 0 mg (■, □), 1 (♦, ◊), 2.5 mg (●, ○), 5 mg (▲, △) and 10 mg (▼, ▽) Printex U soot with NO (2000 ppm) + O_2 (10%) for 300 s. For clarity the CO_2 profiles are displaced to the top of the plot. In all cases the NO + O_2 was switched into the stream at 1 min.

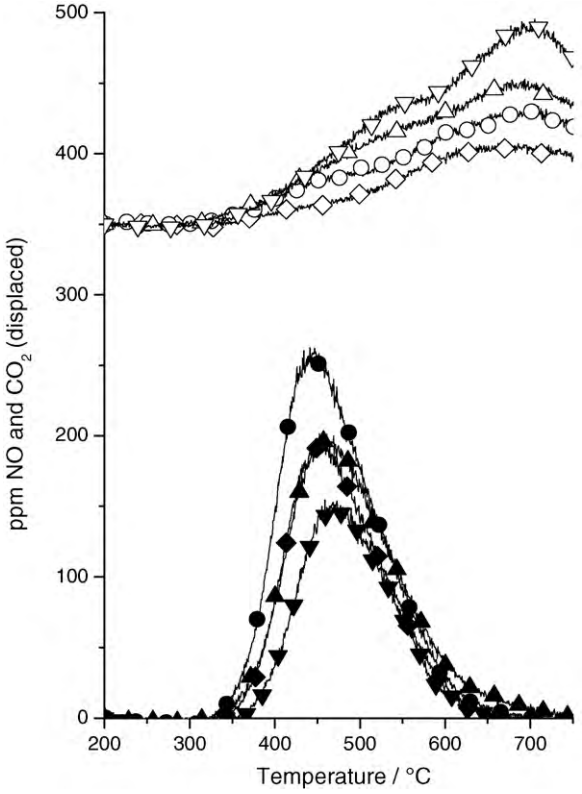

Fig. 6. NO (closed symbols) and CO_2 (open symbols—displaced) profiles during TPD following the dose shown in Fig. 5. 1% Pt/10% BaO/Al_2O_3 mixed with 1 (♦, ◊, 2.5 mg (●, ○) 5 mg (▲, △) and 10 mg (▼, ▽) Printex U soot.

removed there is, in all cases, a relatively small release of NO (not NO_2) from the catalyst and this is the same (although noticeably smaller) feature that was seen in Fig. 1 in the absence of $C_{(s)}$.

As before (Fig. 3) in the presence of soot the levels of NO_2 in the NO_x mixture are far lower than when soot is absent. At the end of a 5 min dose in the absence of soot 18% of the NO_x is NO_2 while in the presence of the various amounts of $C_{(s)}$ this falls to approximately 6%. This is due to the reaction of any formed NO_2 with $C_{(s)}$ and subsequent reformation of NO. There is no systematic relationship between the levels of $C_{(s)}$ in the reaction mixture and the levels of NO_2 in the exhaust gas leaving the reactor.

As expected, the CO_2 profiles seen during the dose of the catalyst–soot mixtures in the presence of different levels of soot do differ in a systematic way from one another. In all cases the production of CO_2 begins once the $NO + O_2$ is switched into the stream, reaches a pseudo-steady-state production after approximately 90 s and ceases as the $NO + O_2$ is removed from the stream. The amounts of CO_2 produced during each experiment varies as a direct function of the amount of $C_{(s)}$ in the catalyst–soot mixture with most being produced when the catalyst:soot ratio is 5:1 (10 mg soot) and least when this is 50:1 (1 mg soot). For reference the CO_2 profile from the initial dose of $NO + O_2$ onto the catalyst in the absence of soot is also shown (!). This confirms that a significant amount of the CO_2 released during the early part of the dose derives from the decomposition of surface $BaCO_3$ rather than the combustion of $C_{(s)}$. The importance of this contribution obviously decreases with time as the surface [$BaCO_3$] which can be displaced in this way is depleted.

The NO and CO_2 profiles recorded during the related TPD experiments are shown in Fig. 6 (No NO_2 was noted during the TPD although again in all cases O_2 desorbed with the same profile as NO). There is no direct correlation between the concentration of soot present in the catalyst–soot admixture and the amount of NO desorbed. While the least amount of NO is desorbed form the 5:1 catalyst–soot mixture (containing 10 mg soot with 50 mg catalyst) the most NO (within the 4 profiles being compared here) is desorbed from the admixture containing 2.5 mg soot (catalyst:soot ratio of 20:1). The maximum temperature of desorption during these experiments ranged from 445 °C to 470 °C (recall, in the absence of soot the maximum temperature of desorption following a 300 s dose was centred at 480 °C).

On the other hand, the extent of the evolved CO_2 profiles again directly follow the concentrations of soot in the catalyst–soot mixtures with the most CO_2 seen from the 5:1 catalyst–soot mixture and the least from the 50:1 mixture. The CO_2 profiles all follow the same shape as seen previously, *i.e.* two desorptions relating to the decomposition of different types of surface $BaCO_3$. While the contribution of liberated $O_2 + C_{(s)}$ cannot be ruled out for the lower temperature formation of CO_2 the shapes of the profiles indicate that any contribution of this reaction is relatively minor, *i.e.* the NO/O_2 profiles peak at different temperatures to the first CO_2 shoulder.

Table 1 shows the amounts of NO_x desorbed from the TPD experiments as a function of dose times and soot concentrations. The nominal proportion of BaO used in storing the NO_x is also shown, although it should be noted that this assumes that all the Ba is present as BaO and available to trap NO_x—a situation we know not to be the case. Nevertheless it provides a useful comparison of the relative amounts of NO_x trapped. It is clear both from the table and the plots in Fig. 6 that, in the presence of soot, the amount of NO_x that this model NSR system can trap is much decreased in the presence of $C_{(s)}$ and the adsorbed NO_x is less stable (as measured by the temperatures of initial and maximum desorption). The latter feature is particularly noticeable when comparing data from the 60 s and 600 s doses and is somewhat less pronounced when the 300 s data is compared. Recall that the NO_x adsorbed in the absence of soot for 300 s was less stable than that adsorbed at 60 s (where the most stable sites are populated) or at 600 s (where we ascribe an increased stability to an extended equilibration between adsorbed NO_x and gas phase NO).

The effect of $C_{(s)}$ in altering the stability of stored NO_x has been noted previously [23] on a Sr-containing NO_x storage system. The reason for this probably relates to surface reactions between $C_{(s)}$ and stored nitrates. These redox reactions would form adsorbed nitrites which would be less stable and therefore decompose at lower temperatures.

The former result, *i.e.* where soot has such a detrimental effect on NO_x adsorption on a model $Pt/BaO/Al_2O_3$ catalysts have been reported previously by Matarrese et al. [22], but only when lower catalyst:soot ratios have been used. These workers noted no impairment of NO_x trapping capacity when catalyst:soot ratios in the range 49:1–9:1 have been used, and a decrease in capacity at very high soot loading (catalyst:soot ratios of 4:1). In contrast, the experiments here detail cases where NO_x trapping is significantly impaired in systems with catalyst:soot ratios as low as 50:1.

We ascribe these conflicting results to the fact that the doses of $NO + O_2$ onto the catalyst–soot mixture in this work were carried out at 400 °C while they were carried out at 350 °C in the cited work. In that case the rate of NO_2 assisted soot combustion would be lower. Reference [21] shows (albeit comparing $T = 300$ °C and 400 °C) an order of magnitude increase in the production of CO_2 from NO_2 promoted soot oxidation (where the NO_2 is formed *in situ* from the oxidation of NO) between these two temperatures. Therefore in the case of the work of Matarrese et al. less formed NO_2 would react with $C_{(s)}$, allowing a greater proportion of the NO_2 to adsorb, react and form stored nitrates. Therefore, the presence of soot would have a lesser impact on NO_x adsorption.

$Pt_{(surf)} + O_2 \rightarrow Pt\text{-}O_{(surf)}$

$NO_{(g)} + Pt\text{-}O_{(surf)} \rightarrow NO_{2(g)} + Pt_{(surf)}$

Route 1

$NO_{2(g)} + BaO \rightarrow \quad \rightarrow \quad \rightarrow \quad Ba(NO_3)_2 \quad (\text{stored } NO_x)$

or

Route 2

$NO_{2(g)} + C_{(s)} \rightarrow CO_{(g)} + NO_{(g)}$

Scheme 1. Proposed mechanism for the $C_{(s)}$ poisoning of the NO_x trapping capacity of a 1% Pt/10% BaO/Al_2O_3 material.

4. Conclusions

In the presence of even small masses of $C_{(s)}$ the amounts of NO_x that a NO_x trap can store in the presence of $NO + O_2$ at 400 °C is decreased considerably. A proposed reason for this is that NO_2 formed on Pt from the $NO + O_2$ reaction is reduced to NO through reaction with soot before it is able to react with BaO and form stable $Ba(NO_3)_2$. A schematic of the proposed mechanism is shown in Scheme 1. The amount of NO_x trapped is not grossly affected by the mass of soot in the catalyst:soot mixture with no systematic change in NO_{xads} levels when catalyst:soot ratios are changed between 50:1 and 5:1.

The adsorbed NO_x also appears to be somewhat less stable (in terms of $T_{initial}$ and T_{max} of the evolved NO TPD profiles) in the presence of soot. We ascribe this to any NO_x adsorbed close to a $C_{(s)}$ particle reacting as the temperature is raised, thereby getting reduced to less stable NO-containing species and desorbing.

One final feature of interest is the fact that this decreased trapping efficiency effect is very pronounced even at very low levels of $C_{(s)}$ in the catalyst:soot mixture, *e.g.* for a sample dosed for 600 s in $NO + O_2$ the trapping efficiency goes from roughly 35% to approximately 9% when 1 mg of soot is added to the catalyst (a 50:1 catalyst:soot ratio). It is not possible, at these low levels of soot, for the soot particles to be in intimate (or even close) proximity to all the BaO available. Visually the mixture is clearly heterogeneous with white catalyst particles being prevalent and discrete black soot particles spread through the catalyst bed. The fact that this small amount of soot which is not in intimate contact with the BaO has such a dramatic effect on the concentration of stored NO_x suggests that there is considerable (either gas phase or surface) mobility in the NO_2 generated on the Pt particles before fixation into $Ba(NO_3)_2$ takes place. This in turn suggests that significant amounts of the NO_x trapping process do not involve a straightforward spill-over of NO_2 from Pt particles to BaO.

Acknowledgements

We gratefully acknowledge funding from EPA Ireland under the STRIVE programme and fellowship funding from the Roberto Rocca Education Program to support PD.

Appendix A. Supplementary data

Supplementary data associated with this article can be found, in the online version, at doi:10.1016/j.apcatb.2010.06.025.

References

[1] L. Castoldi, R. Matarrese, L. Lietti, P. Forzatti, Applied Catalysis B: Environmental 64 (2006) 25–34.
[2] M. Piacentini, M. Maciejewski, A. Baiker, Applied Catalysis B: Environmental 60 (2005) 265–275.
[3] A. Setiabudi, M. Makkee, J.A. Moulijn, Applied Catalysis B: Environmental 42 (2003) 35–45.
[4] J. Oi, A. Obuchi, G.R. Bamwenda, A. Ogata, H. Yagita, S. Kushiyama, K. Mizuno, Applied Catalysis B: Environmental 12 (1997) 277–286.
[5] G.R. Bamwenda, A. Obuchi, A. Ogata, J. Oi, S. Kushiyama, K. Mizuno, Journal of Molecular Catalysis A: Chemical 126 (1997) 151–159.
[6] M. Piacentini, M. Maciejewski, A. Baiker, Topics in Catalysis 42–43 (2007) 55–59.
[7] A. Casapu, J.D. Grunwaldt, M. Maciejewski, F. Krumeich, A. Baiker, M. Wittrock, S. Eckhoff, Applied Catalysis B: Environmental 78 (2008) 288–300.
[8] I. Nova, L. Lietti, P. Forzatti, Catalysis Today 136 (2008) 128–135.
[9] L. Olsson, P. Jozsa, M. Nilsson, E. Jobson, Topics in Catalysis 42–43 (2007) 95–98.
[10] K. Shimizu, Y. Saito, T. Nobukawa, N. Miyoshi, A. Satsuma, Catalysis Today 139 (2008) 24–28.
[11] I. Nova, L. Castoldi, F. Prinetto, V. Dal Santo, L. Lietti, E. Tronconi, P. Forzatti, G. Ghiotti, R. Psaro, S. Recchia, Topics in Catalysis 30–31 (2004) 181–186.
[12] B.R. Kromer, L. Cao, L. Cumaranatunge, S.S. Mulla, J.L. Ratts, A. Yezerets, N.W. Currier, F.H. Ribeiro, W.N. Delgass, J.M. Caruthers, Catalysis Today 136 (2008) 93–103.
[13] U. Hoffmann, T. Rieckmann, J.X. Ma, Chemical Engineering Science 46 (1991) 1101–1113.
[14] B.A.A.L. van Setten, M. Makkee, J.A. Moulijn, Catalysis Reviews—Science and Engineering 43 (2001) 489–564.
[15] P. Ciambelli, P. Corbo, V. Palma, P. Russo, S. Vaccaro, B. Vaglieco, Topics in Catalysis 16 (2001) 279–284.
[16] J.A. Sullivan, O. Keane, L. Maguire, Catalysis Communications 6 (2005) 472–475.
[17] J.A. Sullivan, O. Keane, Catalysis Today 114 (2006) 340–345.
[18] K. Krishna, M. Makkee, Catalysis Today 114 (2006) 48–56.
[19] B.R. Stanmore, J.F. Brilhac, P. Gilot, Carbon 39 (2001) 2247–2268.
[20] A. Setiabudi, M. Makkee, J.A. Moulijn, Applied Catalysis B: Environmental 50 (2004) 185–194.
[21] J.A. Sullivan, O. Keane, A. Cassidy, Applied Catalysis B: Environmental 75 (2007) 102–106.
[22] R. Matarrese, L. Castadoldi, L. Lietti, P. Forzatti, Topics in Catalysis 52 (2009) 2041–2046.
[23] A.L. Kustov, M. Makkee, Applied Catalysis B: Environmental 88 (2009) 263–271.
[24] J.P.A. Neeft, M. Makkee, J.A. Moulijn, Fuel Processing Technology 47 (1996) 1.
[25] Eight Peak Index of Mass Spectra, 3rd ed., Unwin, Surrey, 1983.
[26] I. Nova, L. Lietti, L. Castoldi, E. Tronconi, P. Forzatti, Journal of Catalysis 239 (2006) 244–254.
[27] A. Lindholm, N.W. Currier, E. Fridell, A. Yezerets, L. Olsson, Applied Catalysis B: Environmental 75 (2007) 78–87.
[28] L. Cao, J.L. Ratts, A. Yezerets, N.W. Currier, J.M. Caruthers, F.H. Ribeiro, W.N. Delgass, Industrial & Engineering Chemistry Research 47 (23) (2008) 9006–9017.
[29] P. Forzatti, L. Castoldi, I. Nova, L. Lietti, E. Tronconi, Catalysis Today 117 (1–3) (2006) 316–320.
[30] W.S. Epling, J.E. Parks, G.C. Campbell, A. Yezerets, N.W. Currier, L.E. Campbell, Catalysis Today 96 (1–2) (2004) 21–30.
[31] C.W. Yi, J. Szanyi, Journal of Physical Chemistry C 113 (2009) 2134–2140.
[32] G. Zhou, T. Luo, R.J. Gorte, Applied Catalysis B: Environmental 64 (2006) 88–95.
[33] M. Piacentini, M. Maciejewski, A. Baiker, Applied Catalysis B: Environmental 59 (2005) 187–195.
[34] W.S. Epling, C.H.F. Peden, J. Szanyi, Journal of Physical Chemistry C 112 (2008) 10952–10959.
[35] L. PerierCamby, G. Thomas, Solid State Ionics 93 (1997) 315–320.
[36] N.W. Cant, M.J. Patterson, Catalysis Today 73 (2002) 271–278.